Preparation and Characterization of Spherical Lignocellulose-based Anion Exchanger from Sugarcane Bagasse

Wei Cao,* Hao Li, Yixia Hong, Ziyi Yang, and Minglai Fu

Biosorption is considered a promising technique for removing heavy metals from water. However, a biosorbent is usually prepared in the form of biomass powder that has drawbacks in stability and uniformity. Herein, a spherical lignocellulose-based anion exchanger (LCB-AE) was prepared from sugarcane bagasse through the method of dissolution-regeneration of biomass followed by quaternary ammonium modification. Dissolution-regeneration conditions of raw biomass were optimized, and the prepared materials were characterized by element composition analysis, pore-structure analysis (mercury intrusion porosimetry), scanning electron microscopy (SEM), X-ray photoelectron spectroscopy (XPS), and carbon-13 nuclear magnetic resonance (^{13}C-NMR) analyses. The LCB-AE has a macro-porous structure and a rough surface occupied mainly by quaternary ammonium and hydroxyl groups. Adsorption selectivity of LCB-AE follows the order of $CrO_4^{2-} > PO_4^{3-} > SO_4^{2-} > NO_3^-$, and adsorption isotherms agree well with the Langmuir model, which suggests the experimental exchange abilities are approximately 0.8 to 0.9 mEq/g. These results show that LCB-AE as a new spherical biosorbent has the potential to be used for anions removal from water.

DOI: 10.15376/biores.17.3.3984-4000

Keywords: Sugarcane bagasse; Lignocellulose bead; Anion exchange; Structure characterization; Sorption isotherm

Contact information: Xiamen Key Laboratory of Municipal and Industrial Solid Waste Utilization and Pollution Control, College of Civil Engineering, Huaqiao University, Xiamen, Fujian 361021, PR China;
** Corresponding author: weicao@hqu.edu.cn*

INTRODUCTION

The ion exchange process is a rapid and efficient method for removal and recovery of ionic pollutants from water and wastewater. Ion exchange material plays an important role in determining process efficiency and cost. The desired material needs to have a low cost and high sorption capacity. Further, it ideally ought to be renewable (Bashir *et al.* 2019). Ion exchange resins that originate from polystyrene and polyacrylic acid are popular in water treatment because of their excellent mechanical properties and exchange sorption performance. However, these resins as petrochemical derivatives are expensive, and they face the problem of depletion of petrochemical resources. Many industries are committed to develop alternative products to reduce the use of petrochemical resources, thereby helping to cope with climate change and reduce carbon emissions.

Over recent decades, a great deal of research has been motivated by the need to develop novel, low-cost, and efficient ion exchangers for separating ionic species from wastewater. Both organic and inorganic materials are involved, such as functional zeolites, double layer hydroxides, cellulose- and chitin-based materials, and metal-organic frameworks (MOFs) (Kim and Kuga 2002; Liang *et al.* 2013; De Gisi *et al.* 2016). A cellulose-based exchanger has been considered as an important alternative of ion exchange resins because cellulose is the most abundant natural polymer in the earth (Hokkanen *et al.* 2016). Additionally, the presence of many hydroxyl groups in its structure makes chemical modifications available. To prepare an anion exchanger, amine and quaternary ammonium groups must be introduced into the cellulose structure to form positively charged sorption sites (Gao *et al.* 2009; Cao *et al.* 2016; Hokkanen *et al.* 2016). Several anion exchangers based on cellulose or cellulose derivatives have been successfully developed previously, and related commercial products have been established, such as the Whatman DE series. Although the exchange capacity of cellulose-based anion exchanger is less than that of commercial polystyrene and polyacrylic resins, it shows good potential for protein separation and in the field of chromatographic analysis (Hokkanen *et al.* 2016). However, it has limitations for application in wastewater treatment, for which it is desirable that the treatment cost be as low as possible. The main challenge may be that cellulose extraction and purification from lignocellulosic biomass are too complicated and costly, making it not available in large quantities for water treatment. Considering wastewater treatment does not require the use of pure cellulose material, researchers turned to raw natural cellulosic materials, especially lignocellulosic biomass wastes, which may have almost no cost (Tran *et al.* 2019).

Therefore, rice straw, corn stalk, wheat straw, walnut, and other agricultural residues are becoming increasingly attractive as new biosorbents for removing aquatic pollutants, in particular heavy metals, because they are abundant, have low cost, and are renewable annually. Generally, crop straw is a type of lignocellulose material, mainly containing cellulose, lignin, and hemicellulose. To convert crop straw into anion sorbent, it needs to be washed and ground, followed by chemical modifications based on hydroxyl group, which is similar to non-homogeneous modification of cellulose. In earlier times, Laszlo reported an anion sorbent with amine groups prepared from sugarcane bagasse powders (Laszlo 1996). Subsequently, rice hull, soy beans, corn stalk, wheat straw, and peanut shell were also selected for preparing anion biosorbents after modification with triethylamine, trimethylamine, or quaternary ammonium salts, *i.e.*, trimethyl dihydroxypropyl ammonium chloride (Marshall and Wartelle 2004; Anirudhan *et al.* 2006; Blagojev *et al.* 2021). These low-cost anion biosorbents exhibit good potential for removing anionic pollutants, such as nitrate, sulfate, phosphate, arsenate, and chromate from wastewater. In the authors' previous studies, anion biosorbents from rice straw and corn stalk were also prepared, and they were used to remove sulfate and chromate from aqueous solution (Cao *et al.* 2011, 2018). However, some drawbacks of biosorbents were observed in previous reports and the authors' own experiments. Most biosorbents were prepared in the form of biomass powder, which has limitations in dynamic adsorption and repeated use because of the lack of stability and uniformity. A fine particle means large hydraulic resistance in bed operation and lacks sufficient mechanical strength in repeated regeneration-adsorption cycles. Apart from lab trials, this may be the main reason behind why few practical applications of biosorbent have been reported in wastewater treatment. The other problem for a powder biosorbent is stability. It has been demonstrated that some organic components of biosorbent powder could be dissolved into solution during the adsorption process (Cao *et al.* 2018; Wen *et al.* 2018). In the authors' own experiment, a sorbent prepared from rice straw particles started to degrade after a month at an extreme situation (anaerobic expanded bed operation). Based on the above analysis, the authors believe that the key to biosorption technique is to develop biosorbents having a similar morphology and stability as the commercial resins in present use.

Therefore, the authors consider the conversion of raw lignocellulosic biomass into spherical beads, which can be used as precursors to produce anion exchangers. The most difficult part is dissolution and regeneration of total components of lignocellulosic biomass in a clean and sustainable way (Huang *et al.* 2019). Ionic liquids makes it possible for natural lignocellulosic materials, such as crop straw, to be shaped into an ideal form without the extraction and purification process of cellulose. Recent studies (Chen *et al.* 2016; Wang *et al.* 2017; Huang *et al.* 2019) showed that ionic liquid could dissolve wood or straw powders directly and then the lignocellulose can be regenerated in the form of short fibers containing much higher cellulose than that of the raw material.

In the present work, sugarcane bagasse was dissolved using an ionic liquid solvent for preparation of lignocellulose bead (LCB), which subsequently was modified into an anion exchanger with epichlorohydrin and trimethylamine in a pyridine reaction system. Synthesis conditions of LCB were optimized with single factor experiments. Elemental analysis, mercury intrusion porosimetry (MIP), scanning electron microscopy (SEM), carbon-13 nuclear magnetic resonance (^{13}C-NMR), and X-ray photoelectron spectroscopy (XPS) were employed to characterize the physicochemical structure of prepared materials. Adsorption performance of LCB-AE was also measured by batch adsorption experiments, including adsorption isotherms and the selectivity for common anions, in order to evaluate its application potential.

EXPERIMENTAL

Materials and Chemicals

Sugarcane bagasse was collected from a fresh sugarcane juice shop located at Jimei District, Xiamen, Fujian Province, China. Raw material was cleaned with tap water, and dried at 60 °C. Then, it was ground to obtain biomass particles with 40- to 80-mesh size using a plant disintegrator. The biomass particles were subsequently ground with a ball grinder for 2 h to achieve a powder consistency, which was used to prepare lignocellulose beads in this work.

Ionic liquid, 1-allyl-3-methylimidazolium chloride ([Amim]Cl), with a purity of more than 98%, was bought from Lanzhou Institute of Chemical Physics (Lanzhou, China). Other chemicals used in this study, such as sodium dicarbonate ($NaHCO_3$), pyridine, dimethylformamide (DFM), trimethylamine, epichlorohydrin (ECH), ethanol, sodium hydroxide (NaOH), and hydrochloric (HCl), were purchased from Sinopharm Chemical Reagent Co., Ltd. (Shanghai, China). All the reagents were of analytical grade.

Preparation of LCB

A certain weight of sugarcane bagasse powder was dissolved in [Amim]Cl solvent under optimized temperature and time conditions. The mass ratio of sugarcane bagasse to [Amim]Cl solvent should be controlled at approximately 3%, as suggested by the authors' pre-experiments. When sugarcane bagasse is completely dissolved in ionic liquid, the yielded viscose liquid is a homogeneous solution with slight brown color. Then, the solution was injected dropwise into a water coagulation bath using a syringe to form spherical lignocellulose beads (LCBs) under a low-speed stirring conditions (50 rpm). After consolidation, the formed LCBs were separated from the water coagulation bath and washed with large volumes of deionized water. The beads can be dried at 60 °C to obtain dry samples for calculation of yield and further characterization analysis. In addition, when a pore-forming agent, $NaHCO_3$, was added to sugarcane bagasse/[Amim]Cl solution, the water coagulation bath needs to be substituted by 0.1 M HCl solution to improve the pore structure of LCB.

Preparation of LCB-AE

Surface chemical modification was conducted with the LCBs for preparing spherical lignocellulose-based anion exchanger. According to previous studies (Cao *et al.* 2016; Hokkanen *et al.* 2016) and preliminary experiments, relative optimal reaction steps and conditions were adopted and described in the following implementation case. First, the LCB (0.2 g) was reacted with ECH (3 mL) in a four-neck flask, which was loaded with DFM as solvent and a little pyridine as catalyst in advance. This reaction step was continued for 1 h at 65 °C. Then, trimethylamine solution (5 mL) was added into the flask, and the reaction remained for 3 h at 100 °C. After separation, the solid product was washed by ethanol solution (1:1), NaOH solution (0.1 M), HCl solution (0.1 M), and deionized water in that order. Consequently, the final product as LCB-AE was converted into Cl^--resident form. The expected reaction route based on hydroxyl groups in lignocellulose structure for preparing LCB-AE is schematically shown in Fig. 1.

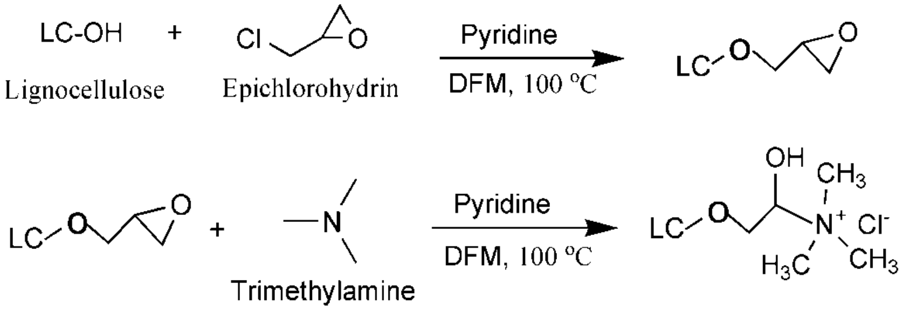

Fig. 1. The expected synthetic route of LCB-AE based on hydroxyl groups in lignocellulose structure

Characterization Methods

Total nitrogen contents (*N* %) of LCB and LCB-AE were determined by Vario EL III element analyzer (Elementar Co., Ltd., Germany) with CHNS pattern. Mercury intrusion porosimetry (MIP) was used to measure the pore structure of the prepared materials. The MIP experiments were conducted using an AutoPore IV 9500 (Micromeritics Instrument Corporation, USA). The main operation parameters included a sample weight 0.035 g, penetrometer volume of 5 mL, Hg-contacting angle 130°, low pressure 0.52 psia, and high pressure 33000 psia with both equilibrium time of 10 s. Scanning electron microscopy was used to probe the surface morphology of prepared materials. The experiment equipment is a field emission SEM (Sigma 300, Carl Zeiss, Germany). X-ray photoelectron spectroscopy was used to probe surface composition and group structure of the prepared materials. The experiments were conducted on an X-ray scanning micro-prober photoelectronic energy spectrometer (Quantum2000, Physical electronics Co., Ltd., USA). The X-ray source was a monochromatic Al K-alpha radiation anode target. The survey spectra and high-resolution spectra were recorded with constant pass energy of 150 and 50 eV, respectively. The XPS determination depth was approximately 0.5 to 7.5 nm. The XPS data were calibrated with C1s peak at 285.0 eV. The high-resolution XPS spectra were decomposed into sub-components, and the curve fitting deviation should be as little as possible. Solid-state ^{13}C nuclear magnetic resonance was used to probe the cellulose structure of the prepared materials. Experiments were performed on a Bruker AVANCE 400 spectrometer (Bruker Co., Ltd., Fällanden Switzerland) with static field strength of 2.3 T (100 MHz 1H) at 298 K. The proton 908 pulse time was 5.5 ms. The acquisition time was 0.03 s and the delay time after acquisition of signals was 3 Ys. The chemical shift data were calibrated with methyl group (methyl benzene) resonance peak at 17.3 ppm.

Batch Adsorption Experiment

Batch adsorption experiments were used to determine adsorption isotherms of LCB-AE for anion species such as sulfate, chromate, nitrate, and phosphate. Adsorption was conducted in a 100 mL conical flask containing 0.1 g LCB-AE and 50 mL solution containing selected anions. The flasks were put into an orbital shaker at conditions of 150 rpm and 25 °C. In batch adsorption experiments, all of the samples were duplicated. After shaking for 24 h, the supernatant liquid was separated from adsorbents by filtration, and the filtrate was collected for chemical analysis. Concentrations of the anions were measured using the ion chromatography method. In addition, chromate was tested using a classic spectrophotometry method (UV-6000, Shanghai Metash Instrument Co., Ltd., Shanghai China) at 540 nm. The selectivity of LCB-AE toward different anions was evaluated by adsorption experiment with a multi-component solution of sulfate, chromate, nitrate, and phosphate anions.

RESULTS AND DISCUSSION

Optimization of LCB Preparation Conditions

Sugarcane bagasse was dissolved in an ionic liquid, [Amim]Cl, under different temperature and time conditions. The dissolution-regeneration results are shown in Table S1. The higher LCB yield was obtained at dissolution time of 1 h and temperature of 110 °C under a certain ratio (3%) of sugarcane bagasse to [Amim]Cl. Compared to previous reports (Sun *et al.* 2012; Chen *et al.* 2016), the pre-treatment process of raw biomass was simplified in this study, *i.e.*, the extraction step with benzene-ethanol solvent was omitted. The experiment suggests that sugarcane bagasse powder also can be dissolved well in the ionic liquid without extraction pre-treatment, and LCB can be prepared in a relatively green and simply way. Under excessively high temperature or prolonged dissolution time, lignocellulose will degrade, and the color of the resulting solution will be dark brown. Previous studies showed the popular dissolution mechanism of cellulose in liquid solution is deconstruction of hydrogen bond by the cation ions from ionic liquid (Kosan *et al.* 2008; Li *et al.* 2018). Dissolution of sugarcane bagasse has a similar mechanism, but it is more difficult. This is because lignocellulose material has a more complicated structure than pure cellulose, since it contains cellulose, lignin, and hemicellulose. Moreover, these components combine into a more complex structure through intermolecular interaction (mainly hydrogen bonds) to form the plant cell wall (Moyer *et al.* 2018; Huang *et al.* 2019).

Different coagulation baths including acetone, acetone aqueous solution (1:1), water, cold water, and ethanol (95%) were tested to prepare LCB. Photos were taken immediately after formation of LCBs in a beaker, as shown in Fig. S1. Results show that sugarcane bagasse lignocellulose could not be regenerated into spherical beads in acetone and even in 1:1 acetone water. Loose granular flocs are observed when ethanol was used as coagulation bath. Beads that have pale yellow color, clear border, and solid feel could be obtained by using water or cold water as coagulation bath. Thus, water is a good and economical coagulation bath for preparing LCB. This result also shows that regeneration of lignocellulose is similar to that of pure cellulose, implying that shaping techniques of cellulose, such as droplet and dispersion, can be tried (Gericke *et al.* 2013).

Basic Physicochemical Properties

Basic physicochemical properties of LCB and LCB-AE are summarized in Table 1, including bead size, color, density, pH point of zero charge (pH_{pzc}), and the contents of cellulose, hemicellulose, and lignin. The prepared LCB is spherical with faint yellow color. It is like a small soybean and has an average diameter of 2.2 mm. The LCB-AE had a light brown color and was the same diameter as the LCB. From the wet density, it can be seen that both LCB and LCB-AE were denser than water when fully wetted. After modification, LCB-AE had a higher pH_{pzc}, which can be attributed to the introduction of protonated ammonium groups, which will be confirmed by subsequent characterization. It is believed that the increase of pH_{pzc} is beneficial for removal of anionic species over a wider range of pH conditions, suggesting LCB-AE is more suitable for anion removal from water. When comparing the components between raw sugarcane bagasse and LCB, it can be found that cellulose and hemicellulose contents slightly increased after dissolution-regeneration process, whereas lignin decreased. This phenomenon is consistent with the findings reported in the previous studies (Zhang *et al.* 2016). It should be noted that the ash content was relatively high, which may have resulted from the insufficient combustion of the acid insoluble matter in the test.

Table 1. Basic Physicochemical Properties of LCB and LCB-AE

Sample	Diameter (mm)	Color	Wet Density (g/cm^3)	pH_{pzc}	Components (%)			
					Cellulose	Lignin	Hemicellulose	Ash
Sugarcane bagasse	< 0.43	Greyish white	1.12	4.4	33.04	4.51	38.79	23.66
LCB	2.2	Faint yellow	1.48	4.7	36.30	3.90	47.88	11.92
LCB-AE	2.2	Light brown	1.41	5.3	ND	ND	ND	ND

ND: Not determined

Pore Structures Characterization by MIP

To improve the pore structure of LCB, a pore-forming agent was used. During dissolution of sugarcane bagasse, $NaHCO_3$ was added into ionic liquid, and correspondingly the water coagulation bath was replaced with a diluted HCl solution. The purpose was to produce carbon dioxide during regeneration and solidification process of lignocellulose, which is helpful to form a porous structure in LCB material. The MIP characterization results for LCB prepared with and without pore-forming agent are both shown in Table 2. Total intrusion volume of LCB almost doubled using the pore-forming agent, and the porosity and apparent density also increased remarkably. The increase of density may be attributed to the loading of $NaHCO_3$, which has a much higher density than lignocellulose. It was also observed that the average pore diameter increased from 3808 to 7255 nm, indicating that the main effect of pore-forming agent was to produce macropores. According to a general classification, pores in material are distinguished based on their diameter as micropores (< 2 nm), mesopores (2 to50 nm), and macropores (> 50 nm). The LCB in the present work had similar density (g/cm^3) and porosity (%) with a reported wheat straw-based lignocellulose bead, but much larger pore diameter and volume (Zhang *et al.* 2016). It should be noted that LCB-AE had a lower total intrusion volume and pore area than LCB, implying that chemical modification may block the pores and reduce the pore area and volume.

Table 2. Summary of MIP Characterization for LCB and LCB-AE

Sample	Total Intrusion Volume (mL/g)	Total Pore Area (m^2/g)	Average Pore Diameter (μm)	Apparent Density (g/cm^3)	Porosity (%)
LCB without pore-forming agent	3.29	3.46	3.81	0.41	57.36
LCB with pore-forming agent	6.08	3.35	7.26	1.03	81.54
LCB-AE	3.97	1.93	8.21	1.03	80.28

Morphology Observation by SEM

General images of sugarcane bagasse, LCB, and LCB-AE were taken by cell phone, and these are shown in Fig. S2. The SEM images of LCB and LCB-AE with different magnifications are shown Fig. 2. It can be seen from Fig. 2a and 2c that both LCB and LCB-AE have coarse surface that consisted of many thin fragment structures and aperture gaps. The fragments were possibly made of regenerated lignocellulose from dissolved sugarcane bagasse. From higher magnifications, the thin fragments of LCB were smooth and flat, as shown in Fig. 2c, whereas they became rough and covered with microparticles in LCB-AE, as shown in Fig. 2d. The microparticles had diameters in the range of 1 to 3 μm, and their element compositions measured by SEM-EDS (atom fraction) were mainly carbon (71.58%), oxygen (17.53%), nitrogen (9.02%), and chlorine (1.87%).

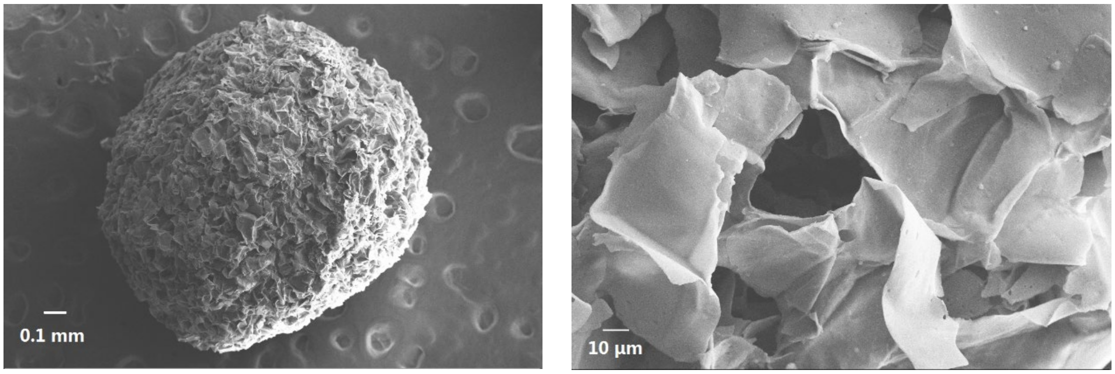

(a) LCB × 30 **(b)** LCB × 500

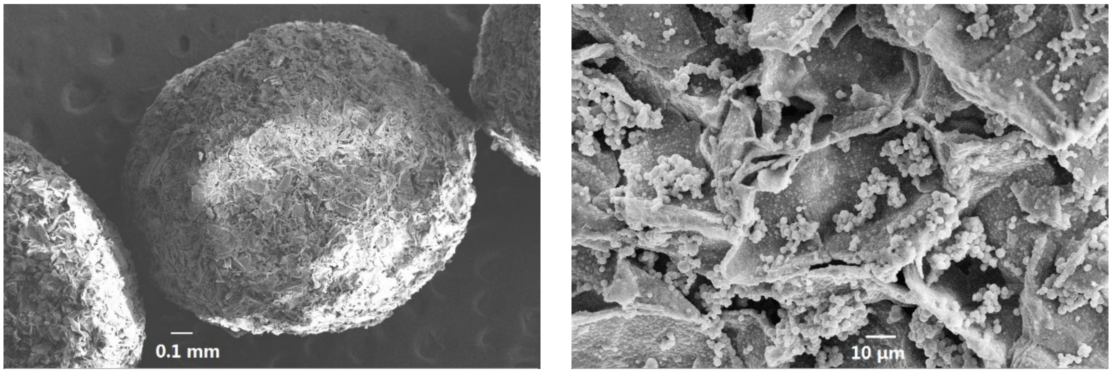

(c) LCB-AE × 30 **(d)** LCB-AE × 500

Fig. 2. SEM images of LCB and LCB-AE

Elemental Composition and TEC of LCB-AE

Total element compositions of LCB and LCB-AE were determined by elementary analysis with CHNS pattern. The results are shown in Table 3. Clearly, LCB-AE has much more nitrogen element than LCB, suggesting N-containing groups were introduced into the material during modification process. Considering the result of SEM-EDS analysis, the introduced groups were mainly concentrated on the surface of LCB-AE. According to nitrogen content, the theoretical anion exchange capacity of anion exchanger can be calculated following Eq. 1,

$$TEC(\mathrm{mEq/g}) = \frac{\mathrm{N\%}}{14 \times 10^{-3}} \tag{1}$$

where N% is the nitrogen content in weight percentage. The *TEC* of LCB-AE was calculated as 1.63 mEq/g. This value is analogous to *TEC* of reported lignocellulose-based anion sorbent such as quaternary ammonium modified wheat straw (Gao *et al.* 2009), rice straw (Cao *et al.* 2011), sugarcane bagasse (Laszlo 1996; Wen *et al.* 2018), and soy hulls (Marshall and Wartelle 2004). This result suggests that regeneration and shaping of lignocellulosic biomass did not have much effect on its quaternization modification efficiency. The *TEC* of LCB-AE was also close to that of pure cellulose-based anion exchangers, such as a diethylamine modified cellulose sorbent (Anirudhan *et al.* 2009), and commercial products such as Whatman DE series and QA52 that have approximately 1.0 mEq/g anion exchange capacity (Marshall *et al.* 2004). It needs to be pointed out that LCB-AE had a much lower *TEC* in contrast to commercial polystyrene-based anion exchangers that generally have exchange capacity of 3 to 4 mEq/g. However, lignocellulosic materials have lower cost and better environmental compatibility compared with petrochemical derivatives.

Table 3. Total and Surface Element Analysis of LCB and LCB-AE

Materials	**Total** Element Composition (%)			**Surface** Element Composition (%)*			
	C	H	N	C 1s	O 1s	N 1s	Cl 2p
LCB	42.33	6.34	0.35	62.42	34.55	2.71	0.34
LCB-AE	45.05	6.63	2.28	72.17	18.14	6.14	3.55

*: Surface element compositions were measured by XPS

XPS Analysis

The XPS survey spectra provides surface element information of LCB and LCB-AE, which are also summarized in Table 3. It is apparent that nitrogen content increased on the surface of LCB-AE, suggesting N-containing groups had been successfully introduced into LCB surface, as expected. The appearance of chlorine element in LCB-AE originated from the soaking process with HCl solution, which can transform the anion exchanger into Cl^--resident form.

High-resolution XPS C1s and N1s spectra of LCB and LCB-AE were achieved in scanned models. As shown in Fig. 3a and 3c, C1s high-resolution spectra were fitted to three components including an intensive peak at binding energy of 284.5 eV, a peak around 285.8 eV, and a relatively weak band around 287.0 eV. The peak at 284.5 eV is related to C-C/C-H bonds in hydrocarbons, particularly methyl and methylene groups from the lignocelluloses structure (Tang *et al.* 2016; Gu *et al.* 2019). The band around 287.0 eV is assigned to carbonyl groups (C=O) and O-C-O linkages in ketones and carboxyl groups in lignocellulose structure (Tang *et al.* 2016; Gu *et al.* 2019). The peak around 285.8 eV is usually attributed to C-O bonds in hydroxyl (C-OH) and ether (C-O-C) groups (Tang *et al.* 2016; Gu *et al.* 2019). Table 4 shows the identification and quantification of C-groups from the high-resolution XPS C1s spectra. The atom fraction of different C-groups in the surface of LCB changes after quaternization modification, while the corresponding peak positions of binding energy are relatively stable. The proportion of C-C/C-H and C=O/O-C-O bonds decreased after modification, while an increase in the amount of C-N/C-OH/C-O-C linkages was observed. This can be attributed to the formation of epoxypropyl-cellulose in the second step of modification process, which increased the amount of ethers and hydroxyl groups in the surface of LCB-AE. Furthermore, the quaternization reaction introduced many C-N bonds into material surface, which can also enhance the peak around 286 eV in XPS C1s spectra of LCB-AE (Cao *et al.* 2016).

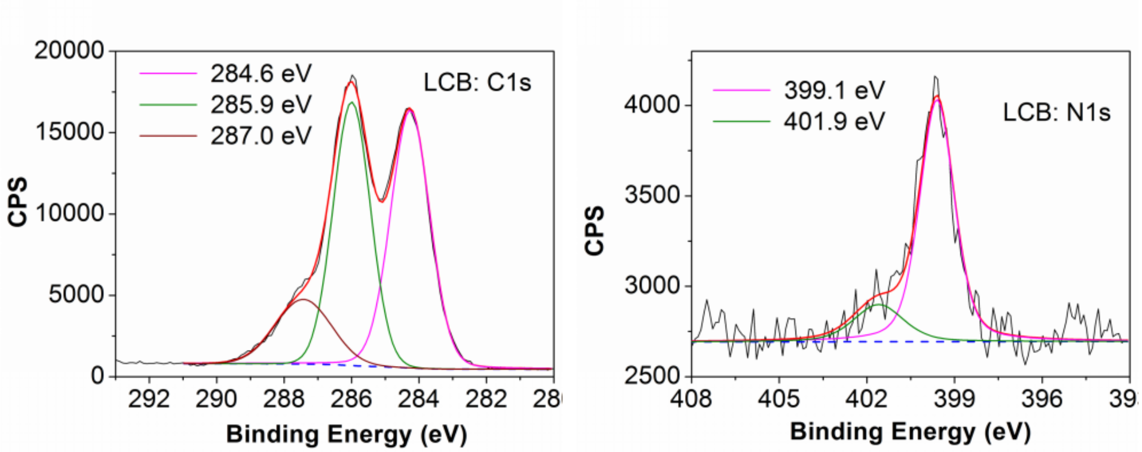

(a) **(b)**

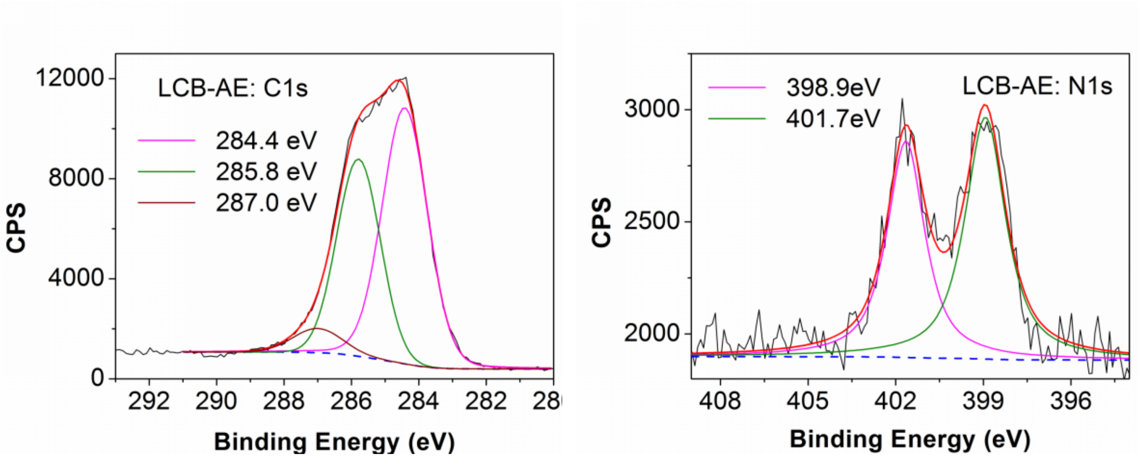

(c) (d)

Fig. 3. The high-resolution XPS C1s spectra of LCB and LCB-AE

Table 4. Identification and Quantification of C- and N-groups in Surface of LCB and LCB-AE

Materials	C-groups						N-groups			
	C-C/C-H		C-N/C-OH/C-O-C		C=O/O-C-O		$-N(CH)_2/-NH_2$		$-N(CH_3)_3^+/-NH_3^+$	
	BE[a](eV)	AF[b](%)	BE(eV)	AF(%)	BE(eV)	AF(%)	BE(eV)	AF(%)	BE(eV)	AF(%)
LCB	284.56	57.53	285.90	30.41	287.03	12.06	399.60	81.84	401.60	18.16
LCB-AE	284.41	55.42	285.79	39.12	287.00	5.46	398.93	54.73	401.65	45.27

a: binding energy; b: atom fraction

The high-resolution XPS N1s spectra of LCB and LAB-AE and their fitting curves are shown in Fig. 3b and 3d. The XPS N1s spectrum is often fitted into two peaks, which are assigned to free amino groups ($-N(CH)_2/-NH_2$) around 399.2 eV and the protonated amino groups ($-N(CH_3)_3^+$) at 401.6 eV (Jansen and van Bekkum 1995; Ederer *et al.* 2017). The atom fraction of free and protonated groups for LCB and LCB-AE are also summarized in Table 4. As shown, most of amino groups in the surface of LCB were free amino groups ($-N(CH)_2/-NH_2$), which probably originated from N-containing compounds in sugarcane bagasse such as protein. The proportion of protonated amino groups of LCB-AE increased remarkably in contrast to LCB, due to that quaternization modification of LCB with trimethylamine introduced the protonated amino groups. Protonation of amines also can be resulted from the hydrogen bonding or interaction of free amino groups with lignocellulose substrate (Zafar *et al.* 2012). It needs to pointed out that amino groups, especially protonated amino groups, are responsible for efficient removal of anionic species. Therefore, LCB-AE with more protonated amino groups shows the potential to be used as an anion exchanger.

^{13}C-NMR spectra

Figure 4 shows the solid state ^{13}C-NMR spectra of LCB and LCB-AE. The adsorption bands from 60 to 110 ppm both in LCB and LCB-AE had the same position and similar shape, which are believed to be from carbon atoms in cellulose structure from C1 to C6. According to previous studies (Fu *et al.* 2015; Kono *et al.* 2016; Khiari *et al.* 2017), the sharp peak at 105 ppm is related to C1 of cellulose, and the two peaks at 83 and 88 ppm are respectively attributed to C4 of amorphous and crystalline cellulose. The strongest signal bands from 72 to 75 ppm are attributed to C2, C3, and C5, and the peaks around 64 ppm arise from C6 of crystalline cellulose. Comparing the ^{13}C-NMR spectra of LCB and LCB-AE, it can be seen that the curve profile and peak positions for C1 through C6 were consistent, implying quaternary ammonium modification had little effect on cellulose crystal structure. It is noticed that there was a new peak at 55 ppm in spectra of LCB-AE. This peak originated from carbon atoms linked to quaternary ammonium groups ($C\text{-}N(CH3)_3$) according to previous studies (Sun *et al.* 2006; Cao *et al.* 2016). This result confirms the presence of quaternary ammonium group in LCB-AE, which is in agreement with characterization result of XPS N1s spectrum.

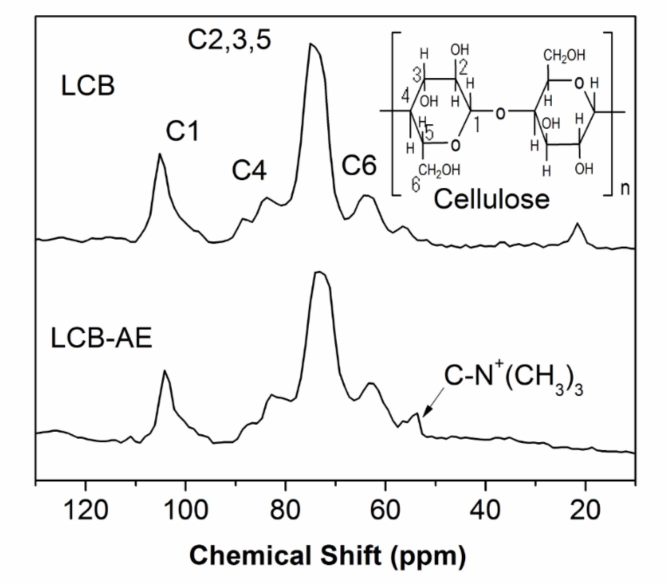

Fig. 4. The ^{13}C NMR spectra of LCB and LCB-AE

Anions Sorption Performance

Sorption isotherms of sulphate (SO_4^{2-}), phosphate (PO_4^{3-}), nitrate (NO_3^-), and chromate (CrO_4^{2-}) anions on LCB-AE are shown in Fig. 5. Under experimental conditions, LCB-AE exhibited good removal for the anions with adsorption amounts in the range of 30 to 50 mg/g. The experimental data were further analyzed with Langmuir and Freundlich adsorption models as expressed in Eqs. 2 and 3, respectively (Wang *et al.* 2019).

$$q_e = q_m K_L C_e /(1 + K_L) \tag{2}$$

$$q_e = K_F (C_e)^{1/n} \tag{3}$$

where q_e (mg/g) and C_e (mg/L) are sorption amount and adsorbate concentration at equilibrium, respectively; q_m (mg/g) represents the maximum sorption capacity for Langmuir adsorption model; K_L (L/mg) and K_F (mg/g) are constants corresponding to Langmuir and Freundlich equations, respectively; and n is a dimensionless constant for Freundlich equation. The Langmuir model is a theoretical equation based on single molecular layer adsorption on homogeneous surface, whereas the Freundlich model is a semiempirical equation for describing heterogeneous surface adsorption (Wang *et al.* 2019).

As shown in Fig. 5, it is clear that the Langmuir model described the experimental data much better than the Freundlich model for the sorption of sulphate, chromate, and nitrate on LCB-AE, while the Freundlich model achieved a higher coefficient of determination (R^2) for phosphate adsorption. The maximum sorption capacities (q_m) calculated from Langmuir isotherm model were 47.28, 39.63, 51.60 mg/g for chromate, sulphate, and nitrate, respectively. After converting the unit of sorption amount, the corresponding results were 0.91, 0.41, and 0.82 mmol/g, respectively. Considering that sulphate is a divalent anion and chromate mainly exists as a monovalent anion ($HCrO_4^-$) in neutral solution (Wen *et al.* 2018), it can be estimated that the experimental sorption ability of LCB-AE was approximately 0.8 to 0.9 mEq/g for common anions. This value is comparable to actual exchange capacity of pure cellulose-based anion exchangers, but less than that of commercial polystyrene-based anion exchangers, which is consistent with the comparison result of *TEC* mentioned in the Elemental Composition and TEC of LCB-AE section.

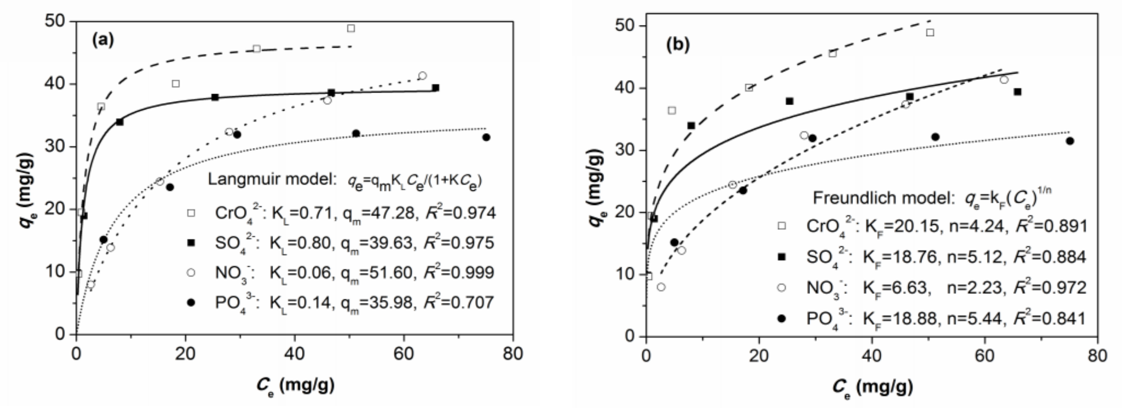

Fig. 5. Adsorption isotherms of CrO_4^{2-}, SO_4^{2-}, NO_3^-, and PO_4^{3-} on LCB-AE: (a) Langmuir model and (b) Freundlich model

To examine the selectivity of LCB-AE, competitive sorption experiments were conducted in a multi-component solution system, which contained CrO_4^{2-}, SO_4^{2-}, PO_3^-, NO_3^-, and Cl^-. The experimental results are summarized in Table 5. Although these anions had almost the same initial concentration, their removal percentages differed noticeably, following the order of $CrO_4^{2-} > PO_4^{3-} > SO_4^{2-} > NO_3^-$. The best sorption was achieved on CrO_4^{2-}, probably because of the occurrence of Cr(VI) reduction to Cr(III) by hydroxyl and carboxyl groups in LCB-AE, which enhances Cr(VI) removal. Previous studies have shown that Cr(VI) could be reduced to Cr(III) by lignocellulose-based materials to some extent (Cao *et al.* 2018; Wen *et al.* 2018). The removal percentage was close for PO_4^{3-} and SO_4^{2-}, whereas it was much lower for NO_3^-. This result suggests that sorption selectivity of monovalent anion on LCB-AE was weaker than that of divalent/trivalent anion, which is consistent with selectivity order of commercial anion exchangers. Table 5 also shows that Cl^- content clearly increased after the sorption experiment, indicating the occurrence of ion exchange between removed anions and Cl^-. Based on a rough estimate, the increase of Cl^- was comparable with the sum of removal quantity of other anions multiplied by their valence state. Thus, ion exchange can be regarded as the main way for sorption of anions by LCB-AE.

Table 5. Competitive Sorption of Common Anions on LCB-AE in a Multi-component Solution

Anions Species	Initial Conc. (mM)	Final Conc. (mM)	Δ (Conc.) (mM)	Removal (%)
CrO_4^{2-}	0.284	0.006	-0.278	97.9
SO_4^{2-}	0.270	0.117	-0.153	56.7
PO_4^{3-}	0.303	0.121	-0.182	60.1
NO_3^-	0.301	0.186	-0.115	38.2
Cl^-	0.330	1.650	+1.320	Increase

The symbol 'Δ (Conc.) ' means the difference between the final and initial concentration

CONCLUSIONS

1. The appropriate preparation conditions of LCBs include a 3% dissolution ratio of biomass to ionic liquid, dissolution temperature and time of 110 °C and 1 h, and water as the coagulation bath. The pore formation method of $NaHCO_3$/diluted HCl coagulation bath can effectively improve macropore structure of LCB.
2. The prepared LCB-AE had a porous structure, a rough surface, a uniform diameter of 2.2 mm, and a pH_{pzc} value of 5.3. The theoretical *TEC* of LCB-AE was calculated as 1.63 mEq/g according to nitrogen content.
3. Both the XPS and ^{13}C-NMR characterizations showed that quaternary ammonium group and hydroxyl group were the main surface groups of LCB-AE.
4. The LCB-AE exhibited good removal to common anions, and sorption selectivity followed the order of $CrO_4^{2-} > PO_4^{3-} > SO_4^{2-} > NO_3^-$. The Sorption isotherms agreed well with Langmuir model, and accordingly the experimental exchange abilities of LCB-AE were estimated as 0.8 to 0.9 mEq/g, which is comparable to actual exchange capacity of pure cellulose-based anion exchangers. The LCB-AE, as a spherical biosorbent, has good potential to be used for removal of anionic pollutants from water.

ACKNOWLEDGEMENTS

This work was supported by the Fundamental Research Funds for the Central Universities (grant number: ZQN-712), the Natural Science Foundation of Fujian Province (grant number: 2021J01283), and the Science and Technology Planning Project of Xiamen City (grant number: 3502Z20203043).

REFERENCES CITED

Anirudhan, T. S., Noeline, B. F., and Manohar, D. M. (2006). "Phosphate removal from wastewaters using a weak anion exchanger prepared from a lignocellulosic residue," *Environmental Science & Technology* 40(8), 2740-2745. DOI: 10.1021/es052070h

Anirudhan, T. S., Jalajamony, S., and Suchithra, P. S. (2009). "Improved performance of a cellulose-based anion exchanger with tertiary amine functionality for the adsorption of chromium(VI) from aqueous solutions," *Colloids and Surfaces A: Physicochemical and Engineering Aspects* 335(1-3), 107-113. DOI: 10.1016/j.colsurfa.2008.10.035

Bashir, A., Malik, L. A., Ahad, S., Manzoor, T., Bhat, M. A., Dar, G. N., and Pandith A. H. (2019). "Removal of heavy metal ions from aqueous system by ion-exchange and biosorption methods," *Environmental Chemistry Letters* 17(2), 729-754. DOI: 10.1007/s10311-018-00828-y

Blagojev, N., Vasić V., Kukić, D., Šćiban, M., Prodanović, J., and Bera, O. (2021). "Modelling and efficiency evaluation of the continuous biosorption of Cu(II) and Cr(VI) from water by agricultural waste materials," *Journal of Environmental Management* 281, article ID 111876. DOI: 10.1016/j.jenvman.2020.111876

Cao, W., Dang, Z., Zhou, X., Yi, X., Wu, P., Zhu, N., and Lu, G. (2011). "Removal of sulphate from aqueous solution using modified rice straw: Preparation, characterization and adsorption performance," *Carbohydrate Polymers* 85(3), 571-577. DOI: 10.1016/j.carbpol.2011.03.016

Cao, W., Wang, Z., Zeng, Q., and Shen, C. (2016). "13C NMR and XPS characterization of anion adsorbent with quaternary ammonium groups prepared from rice straw, corn stalk and sugarcane bagasse," *Applied Surface Science* 389, 404-410. DOI: 10.1016/j.apsusc.2016.07.095

Cao, W., Wang, Z., Ao, H., and Yuan, B. (2018). "Removal of Cr(VI) by corn stalk based anion exchanger: The extent and rate of Cr(VI) reduction as side reaction," *Colloids and Surfaces A: Physicochemical and Engineering Aspects* 539, 424-432. DOI: 10.1016/j.colsurfa.2017.12.049

Chen, M., Zhang, X., Zhang, A., Liu, C., and Sun, R. (2016). "Direct preparation of green and renewable aerogel materials from crude bagasse," *Cellulose* 23(2), 1325-1334. DOI: 10.1007/s10570-015-0814-9

De Gisi, S., Lofrano, G., Grassi, M., and Notarnicola, M. (2016). "Characteristics and adsorption capacities of low-cost sorbents for wastewater treatment: A review," *Sustainable Materials and Technologies* 9, 10-40. DOI: 10.1016/j.susmat.2016.06.002

Ederer, J., Janoš P., Ecorchard P., Tolasz J., Štengl, V., Beneš, H., Perchacz, M., and Pop-Georgievski, O. (2017). "Determination of amino groups on functionalized graphene oxide for polyurethane nanomaterials: XPS quantitation *vs.* functional speciation," *RSC Advances* 7(21), 12464-12473. DOI: 10.1039/C6RA28745J

Fu, L., McCallum, S. A., Miao, J., Hart, C., Tudryn, G. J., Zhang, F., and Linhardt, R. J. (2015). "Rapid and accurate determination of the lignin content of lignocellulosic biomass by solid-state NMR," *Fuel* 141, 39-45. DOI: 10.1016/j.fuel.2014.10.039

Gao, B., Xu, X., Wang, Y., Yue, Q., and Xu, X. (2009). "Preparation and characteristics of quaternary amino anion exchanger from wheat residue," *Journal of Hazardous Materials* 165(1-3), 461-468. DOI: 10.1016/j.jhazmat.2008.10.014

Gericke, M., Trygg, J., and Fardim, P. (2013). "Functional cellulose beads: Preparation, characterization, and applications," *Chemical Reviews* 113(7), 4812-4836. DOI: 10.1021/cr300242j

Gu, L., Jiang, B., Song, J., Jin, Y., and Xiao, H. (2019). "Effect of lignin on performance of lignocellulose nanofibrils for durable superhydrophobic surface," *Cellulose* 26(2), 933-944. DOI: 10.1007/s10570-018-2129-0

Hokkanen, S., Bhatnagar, A., and Sillanpää, M. (2016). "A review on modification methods to cellulose-based adsorbents to improve adsorption capacity," *Water Research* 91, 156-173. DOI: 10.1016/j.watres.2016.01.008

Huang, C., Guo, H. J., Zhang, H. R., Xiong, L., Li, H. L., and Chen, X. D. (2019). "A new concept for total components conversion of lignocellulosic biomass: A promising direction for clean and sustainable production in its bio-refinery," *Journal of Chemical Technology & Biotechnology* 94(8), 2416-2424. DOI: 10.1002/jctb.6086

Jansen, R. J. J., and van Bekkum, H. (1995). "XPS of nitrogen-containing functional groups on activated carbon," *Carbon* 33(8), 1021-1027. DOI: 10.1016/0008-6223(95)00030-H

Khiari, R., Salon, M. B., Mhenni, M. F., Mauret, E., and Belgacem, M. N. (2017). "Synthesis and characterization of cellulose carbonate using greenchemistry: Surface modification of Avicel," *Carbohydrate Polymers* 163, 254-260. DOI: 10.1016/j.carbpol.2017.01.037

Kim, U. J., and Kuga, S. (2002). "Polyallylamine-grafted cellulose gel as high-capacity anion-exchanger," *Journal of Chromatography A* 946(1-2), 283-289. DOI: 10.1016/s0021-9673(01)01512-6

Kono, H., Oshima, K., Hashimoto, H., Shimizu, Y., and Tajima, K. (2016). "NMR characterization of sodium carboxymethyl cellulose 2: Chemical shift assignment and conformation analysis of substituent groups," *Carbohydrate Polymers* 150, 241-249. DOI: 10.1016/j.carbpol.2016.05.003

Kosan, B., Michels, C., and Meister, F. (2008). "Dissolution and forming of cellulose with ionic liquids," *Cellulose* 15(1), 59-66. DOI: 10.1007/s10570-007-9160-x

Laszlo, A. J. (1996). "Preparing an ion exchange resin from sugarcane bagasse to remove reactive dye from wastewater," *Textile Chemist and Colorist* 28(5), 13-17.

Li, Y., Wang, J., Liu, X., and Zhang, S. (2018). "Towards a molecular understanding of cellulose dissolution in ionic liquids: Anion/cation effect, synergistic mechanism and physicochemical aspects," *Chemical Science* 9(17), 4027-4043. DOI: 10.1039/C7SC05392D

Liang, F., Song, Y., Huang, C., Li, Y., and Chen, B. (2013). "Synthesis of novel lignin-based ion-exchange resin and its utilization in heavy metals removal," *Industrial & Engineering Chemistry Research* 52(3), 1267-1274. DOI: 10.1021/ie301863e

Marshall, W. E., and Wartelle, L. H. (2004). "An anion exchange resin from soybean hulls," *Journal of Chemical Technology & Biotechnology* 79(11), 1286-1292. DOI: 10.1002/jctb.1126

Moyer, P., Smith, M. D., Abdoulmoumine, N., Chmely, S. C., Smith, J. C., Petridis, L., and Labbé, N. (2018). "Relationship between lignocellulosic biomass dissolution and physicochemical properties of ionic liquids composed of 3-methylimidazolium cations and carboxylate anions," *Physical Chemistry Chemical Physics* 20(4), 2508-2516. DOI: 10.1039/C7CP07195G

Sun, L., Du, Y., Fan, L., Chen, X., and Yang, J. (2006). "Preparation, characterization and antimicrobial activity of quaternized carboxymethyl chitosan and application as pulp-cap," *Polymer* 47(6), 1796-1804. DOI: 10.1016/j.polymer.2006.01.073

Sun, S., Li, M., Yuan, T., Xu, F., and Sun, R. (2012). "Effect of ionic liquid pretreatment on the structure of hemicelluloses from corncob," *Journal of Agricultural and Food Chemistry* 60(44), 11120-11127. DOI: 10.1021/jf3021464

Tang, R., Zhang, Y., Zhang, Y., and Yu, Z. (2016). "Synthesis and characterization of chitosan based dye containing quaternary ammonium group," *Carbohydrate Polymers* 139, 191-196. DOI: 10.1016/j.carbpol.2015.12.047

Tran, H. N., Nguyen, H. C., Woo, S. H., Nguyen, T. V., Vigneswaran, S., Hosseini-Bandegharaei, A., Rinklebe, J., Kumar Sarmah, A., Ivanets, A., Dotto, G. L., *et* *al.*(2019). "Removal of various contaminants from water by renewable lignocellulose-derived biosorbents: A comprehensive and critical review," *Critical Reviews in Environmental Science and Technology* 49(23), 2155-2219. DOI: 10.1080/10643389.2019.1607442

Wang, J., Boy, R., Nguyen, N. A., Keum, J. K., Cullen, D. A., Chen, J., Soliman, M., Littrell, K. C., Harper, D., Tetard, L., *et al.* (2017). "Controlled assembly of lignocellulosic biomass components and properties of reformed materials," *ACS Sustainable Chemistry & Engineering* 5(9), 8044-8052. DOI: 10.1021/acssuschemeng.7b01639

Wang, H., Wang, B., Li, J., and Zhu, T. (2019). "Adsorption equilibrium and thermodynamics of acetaldehyde/acetone on activated carbon," *Separation and Purification Technology* 209, 535-541. DOI: 10.1016/j.seppur.2018.07.076

Wen, X., Sun, N., Yan, C., Zhou, S., and Pang, T. (2018). "Rapid removal of Cr(VI) ions by densely grafted corn stalk fibers: High adsorption capacity and excellent recyclable property," *Journal of the Taiwan Institute of Chemical Engineers* 89, 95-104. DOI: 10.1016/j.jtice.2018.04.021

Zafar, A., Schjødt-Thomsen, J., Sodhi, R., Goacher, R., and Kubber, D. (2012). "X-ray photoelectron spectroscopy and time-of-flight secondary ion mass spectrometry characterization of aging effects on the mineral fibers treated with aminopropylsilane and quaternary ammonium compounds," *Surface and Interface Analysis* 44(7), 811-818. DOI: 10.1002/sia.4825

Zhang, H., Zhang, Z., and Liu, K. (2016). "Regenerated lignocellulose beads prepared with wheat straw," *BioResources* 11(2), 4281-4294. DOI: 10.15376/biores.11.2.4281-4294

Article submitted: March 11, 2022; Peer review completed: April 26, 2022; Revisions accepted: May 4, 2022; Published: May 6, 2022.
DOI: 10.15376/biores.17.3.3984-4000

APPENDIX

Supplementary Material

Table S1. Effects of Dissolution Time and Temperature on Preparation of LCB

Trial No.	Factors	Factor Levels	LCB Yield (%)	Description
1	Dissolution Time (h)	0.5	123.02	Incomplete dissolution, light brown solution
2		1	155.13	Brown solution
3		1.5	131.27	Dark brown solution
4		2	141.74	Dark brown solution
5	Dissolution Temperature (°C)	90	141.51	Light brown solution
6		100	144.23	Light brown solution
7		110	169.29	Brown solution
8		120	132.49	Dark brown solution

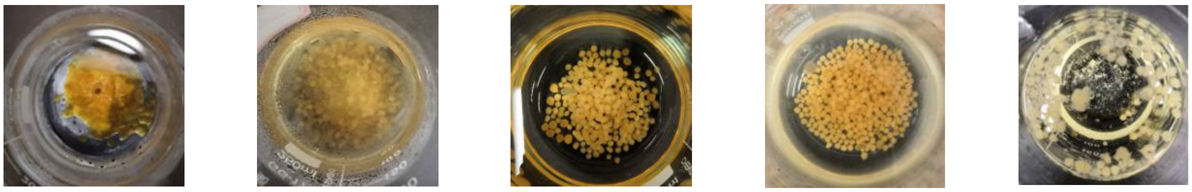

(a) Acetone **(b)** Acetone + Water **(c)** Water **(d)** Cold water (273 K) **(e)** Ethanol

Fig. S1. LCB formation in different coagulation baths

(a) Sugarcane bagasse **(b)** LCB **(c)** LCB-AE

Fig. S2. Material images taken by cellphone camera